EXTENDED PDF FORMAT
SPONSORED BY
Luminex® Multiplex Immunoassays
One simple solution for profiling your complex samples
R&D SYSTEMS >Learn More
www.rndsystems.com

Enhanced Seasonal Exchange of CO_2 by Northern Ecosystems Since 1960

H. D. Graven *et al.*

Science **341**, 1085 (2013);
DOI: 10.1126/science.1239207

This copy is for your personal, non-commercial use only.

If you wish to distribute this article to others, you can order high-quality copies for your colleagues, clients, or customers by clicking here.

Permission to republish or repurpose articles or portions of articles can be obtained by following the guidelines here.

The following resources related to this article are available online at www.sciencemag.org (this information is current as of September 13, 2013):

Updated information and services, including high-resolution figures, can be found in the online version of this article at:
http://www.sciencemag.org/content/341/6150/1085.full.html

Supporting Online Material can be found at:
http://www.sciencemag.org/content/suppl/2013/08/07/science.1239207.DC1.html

A list of selected additional articles on the Science Web sites **related to this article** can be found at:
http://www.sciencemag.org/content/341/6150/1085.full.html#related

This article **cites 63 articles**, 8 of which can be accessed free:
http://www.sciencemag.org/content/341/6150/1085.full.html#ref-list-1

This article has been **cited by** 1 articles hosted by HighWire Press; see:
http://www.sciencemag.org/content/341/6150/1085.full.html#related-urls

Downloaded from www.sciencemag.org on September 13, 2013

Science (print ISSN 0036-8075; online ISSN 1095-9203) is published weekly, except the last week in December, by the American Association for the Advancement of Science, 1200 New York Avenue NW, Washington, DC 20005. Copyright 2013 by the American Association for the Advancement of Science; all rights reserved. The title *Science* is a registered trademark of AAAS.

11. M. L. Lister *et al.*, *Astrophys. J.* **584**, 135–146 (2003).
12. R. Morganti *et al.*, *Astron. Astrophys.* **424**, 119 (2004).
13. J. N. Bahcall, R. D. Ekers, *Astrophys. J.* **157**, 1055 (1969).
14. G. Mellema, J. D. Kurk, H. J. A. Röttgering, *Astron. Astrophys.* **395**, L13–L16 (2002).
15. C. Stanghellini *et al.*, *Astron. Astrophys.* **443**, 891–902 (2005).
16. J. Holt *et al.*, *Mon. Not. R. Astron. Soc.* **370**, 1633–1650 (2006).
17. B. R. McNamara, P. E. J. Nulsen, *New J. Phys.* **14**, 055023 (2012).

Acknowledgments: The European VLBI Network is a joint facility of European, Chinese, South African, and other radio astronomy institutes funded by their national research councils. The National Radio Astronomy Observatory is a facility of the National Science Foundation operated under cooperative agreement by Associated Universities, Inc. J.F. acknowledges the ASTRON/JIVE Summer Student Programme during which she carried out this project. Z.P. acknowledges partial support from the Hungarian Scientific Research Fund, grant OTKA K104539.

13 May 2013; accepted 24 July 2013
10.1126/science.1240436

Enhanced Seasonal Exchange of CO_2 by Northern Ecosystems Since 1960

H. D. Graven,[1]* R. F. Keeling,[1] S. C. Piper,[1] P. K. Patra,[2] B. B. Stephens,[3] S. C. Wofsy,[4] L. R. Welp,[1] C. Sweeney,[5] P. P. Tans,[5] J. J. Kelley,[6] B. C. Daube,[4] E. A. Kort,[7]† G. W. Santoni,[4] J. D. Bent[1]

Seasonal variations of atmospheric carbon dioxide (CO_2) in the Northern Hemisphere have increased since the 1950s, but sparse observations have prevented a clear assessment of the patterns of long-term change and the underlying mechanisms. We compare recent aircraft-based observations of CO_2 above the North Pacific and Arctic Oceans to earlier data from 1958 to 1961 and find that the seasonal amplitude at altitudes of 3 to 6 km increased by 50% for 45° to 90°N but by less than 25% for 10° to 45°N. An increase of 30 to 60% in the seasonal exchange of CO_2 by northern extratropical land ecosystems, focused on boreal forests, is implicated, substantially more than simulated by current land ecosystem models. The observations appear to signal large ecological changes in northern forests and a major shift in the global carbon cycle.

Observations of atmospheric CO_2 concentration from the longest-running Northern Hemisphere records at Mauna Loa, Hawaii (MLO, 20°N) and Barrow, Alaska (BRW, 71°N) show increasing trends in seasonal amplitude (Fig. 1) (*1*–*4*). Shorter records from other ground-based sites in the Northern Hemisphere also show increasing trends in amplitude, with the largest changes at high latitudes (*5*), but the long-term change and especially its spatial pattern have not been well characterized by existing data sets because only MLO and BRW have records extending back to the 1950s and 1960s (*6*–*9*). The two sites show similar trends in the timing of CO_2 drawdown, advancing by roughly 1 week, but differing trends in amplitude: The amplitude at MLO increased by 15 ± 5% over the past 50 years, while the amplitude at BRW increased by at least twice as much (Fig. 1). The best estimate for BRW is a 35% increase in amplitude, with a range of 30 to 49%, including uncertainty from changes in measurement site location, sampling inlet height, and local vegetation effects (*10*, *11*).

Here, we present seasonal CO_2 cycles observed by the recent High-Performance Instrumented Airborne Platform for Environmental Research (HIAPER) Pole-to-Pole Observations (HIPPO) large-scale aircraft campaign (*12*) and regular aircraft profiles over several fixed sites by the National Oceanic and Atmospheric Administration (NOAA) Carbon Cycle Group Aircraft Program from 2009 to 2011 and compare them to observations made 50 years earlier during the International Geophysical Year (IGY) (*13*). The IGY observations were obtained by 160 weather reconnaissance flights above the North Pacific and Arctic Oceans from 1958 to 1961 along 500 and 700 millibar (mb) pressure surfaces (~6 and 3 km altitude). To assess changes in seasonal CO_2 amplitude over time, we examine HIPPO and NOAA data over the same regions and pressure surfaces as the IGY data (*14*). The comparison reveals a strikingly large (~50%) amplitude increase north of 45°N, indicating that major ecological changes must have occurred in northern land ecosystems over the past 50 years.

We calculate an amplitude gain factor for the 1958 to 1961 and 2009 to 2011 observations in 10° latitude bands at 500 and 700 mb after detrending the data by subtracting the observed deseasonalized trend at MLO and after specifying the shape of the seasonal cycle in each pressure and latitude band using fits to the NOAA aircraft data, which have higher temporal resolution than the HIPPO and IGY data (*14*). This method does not allow for the detection of changes in phase, which in any case are not clearly resolvable in the data (*14*), but shifts of up to 7 days as observed at MLO and BRW do not significantly affect the calculation of amplitude (*1*).

An increase in amplitude at least as large as that detected at Barrow is found over a wide range of pressures and at all latitudes north of 45°N (Fig. 2). The change in seasonal CO_2 amplitude north of 45°N is about +5 parts per million (ppm) at all pressures, representing a 57 ± 7% increase at 500 mb since 1958 to 1961 (Figs. 2 and 3) (~0.9 ± 0.1% year^{-1} over 50 years). The seasonal CO_2 amplitude increase is smaller between 35° and 45°N at 500 mb, 26 ± 18%, whereas there is no distinguishable amplitude change south of 35°N (Fig. 2). The same pattern appears at 700 mb, although the IGY data are limited to 10° to 30°N and 65° to 90°N at 700 mb. Low-latitude amplitude changes in the aircraft data are consistent, within their uncertainties, with the surface measurements from Mauna Loa at ~670 mb.

Representativeness of the aircraft data is shown by the similarity between HIPPO and NOAA data for 2009 to 2011 (*15*), and between the IGY and independent data from 1963 to 1968 over the North Atlantic Ocean (*16*). The large changes in amplitude between 1958 to 1963 and 2009 to 2011 north of 45°N (35 to 66%) substantially exceed interannual variation at Barrow (±4%) (Fig. 1) and in high-latitude NOAA aircraft data for recent years (±15%) (*15*), indicating that the observations represent a long-term change rather than a short-term fluctuation.

Fossil fuel, wildfire, and ocean fluxes of CO_2 contribute only a few percent to the seasonal CO_2 cycle in the Northern Hemisphere (*5*, *17*, *18*), limiting their impact on trends in CO_2 amplitude to less than a few percent (*19*). Because midtropospheric amplitude changes north of 45°N are at least as large as those at Barrow, the observations cannot be explained solely by trends in the intensity of vertical mixing (*19*), although changes in transport may cause secondary effects. Model simulations also indicate that potential biases caused by uneven sampling within each latitude band are much smaller than the uncertainties in measured CO_2 amplitude change (*19*).

The large increase in CO_2 amplitude north of 45°N must therefore be attributed almost entirely to the terrestrial biosphere. We now focus on assessing the magnitude and driving factors for trends in the seasonal exchange of CO_2 from net ecosystem production (NEP) by calculating optimal estimates of NEP change that best match

[1]Scripps Institution of Oceanography, University of California, San Diego, La Jolla, CA, USA. [2]Research Institute for Global Change, Yokohama, Japan. [3]National Center for Atmospheric Research, Boulder, CO, USA. [4]School of Engineering and Applied Science, Harvard University, Cambridge, MA, USA. [5]National Oceanic and Atmospheric Administration, Boulder, CO, USA. [6]Institute of Marine Science, University of Alaska, Fairbanks, Fairbanks, AK, USA. [7]Jet Propulsion Laboratory, California Institute of Technology, Pasadena, CA, USA.

*Corresponding author. E-mail: hgraven@ucsd.edu
†Present address: Department of Atmospheric, Oceanic and Space Sciences, University of Michigan, Ann Arbor, MI, USA.

Downloaded from www.sciencemag.org on September 13, 2013

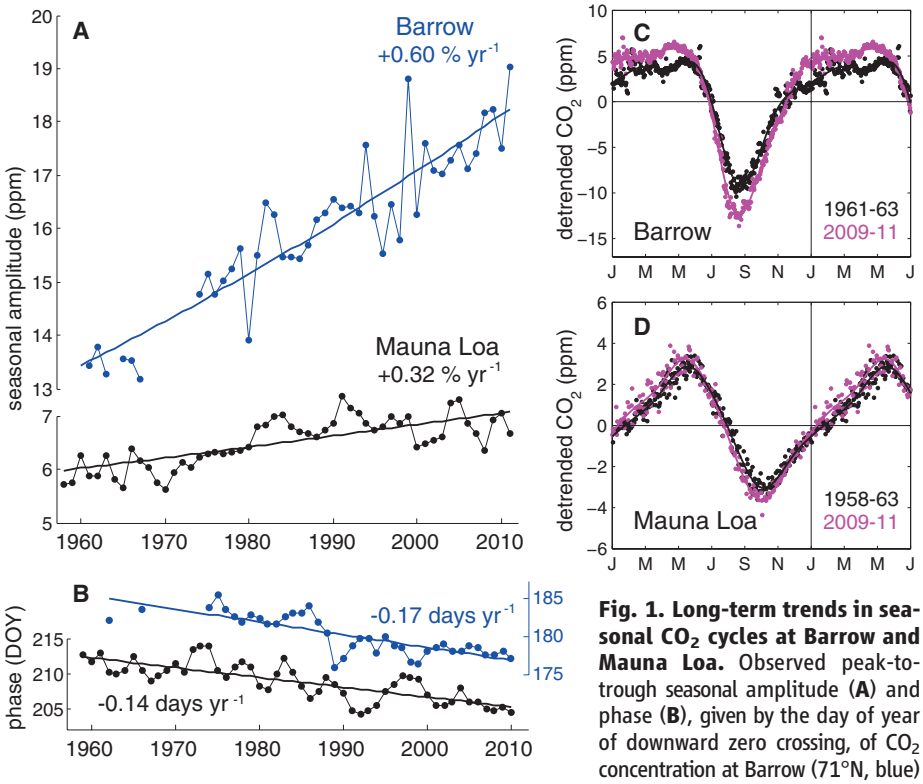

Fig. 1. Long-term trends in seasonal CO_2 cycles at Barrow and Mauna Loa. Observed peak-to-trough seasonal amplitude (**A**) and phase (**B**), given by the day of year of downward zero crossing, of CO_2 concentration at Barrow (71°N, blue) and Mauna Loa (20°N, black) measured by the Scripps CO_2 Program (*7*, *8*) and the NOAA Global Monitoring Division (*9*). Growth rate of amplitude is given in percentage change per year, with 1 SD uncertainty of ±0.05 to 0.07% year^{-1}. Seasonal CO_2 cycles observed at Barrow (**C**) and Mauna Loa (**D**) for the 1961 to 1963 or 1958 to 1963 and 2009 to 2011 time periods. The first 6 months of the year are repeated.

the atmospheric CO_2 amplitude change and then exploring potential mechanisms with historical simulations of terrestrial ecosystem models.

We begin with spatially resolved monthly estimates of NEP averaged over 2005 to 2010 that have been optimized using terrestrial ecosystem model simulations and current observations from the global CO_2 network in two atmospheric transport models, Atmospheric Chemistry Transport Model (ACTM) (*20*) and TM3 (*21*). We simulate separate tracers in ACTM and TM3 representing large regions (Fig. 3C) to assess their contribution to the seasonal CO_2 cycle at different tropospheric locations (Fig. 3, A and B), then we adjust monthly NEP for the large regions by a consistent fraction—that is, by changing the amplitude but not the phase in order to best match the observed CO_2 amplitude changes, roughly centered on 155°W (Fig. 3, D to F) (*22*).

Exploiting our observation that CO_2 amplitude changes are much larger north of 45°N, we optimize changes in NEP in boreal and Arctic regions (Case 1 in Fig. 3, D to F), the regions with stronger influence on CO_2 cycles at high latitudes compared with low latitudes (*5*) (Fig. 3, A and B). Due to isentropic transport, the seasonal cycle at 70°N and 500 mb is less sensitive to the Arctic than to regions farther south (Fig. 3B), showing that changes cannot only be occurring in the Arctic. The optimal uniform change in NEP amplitude in boreal and Arctic regions, fitting to CO_2 amplitude changes north of 45°N only, is an 85% [73 to 107% confidence interval (CI)] (*23*) increase. Extending NEP changes to include

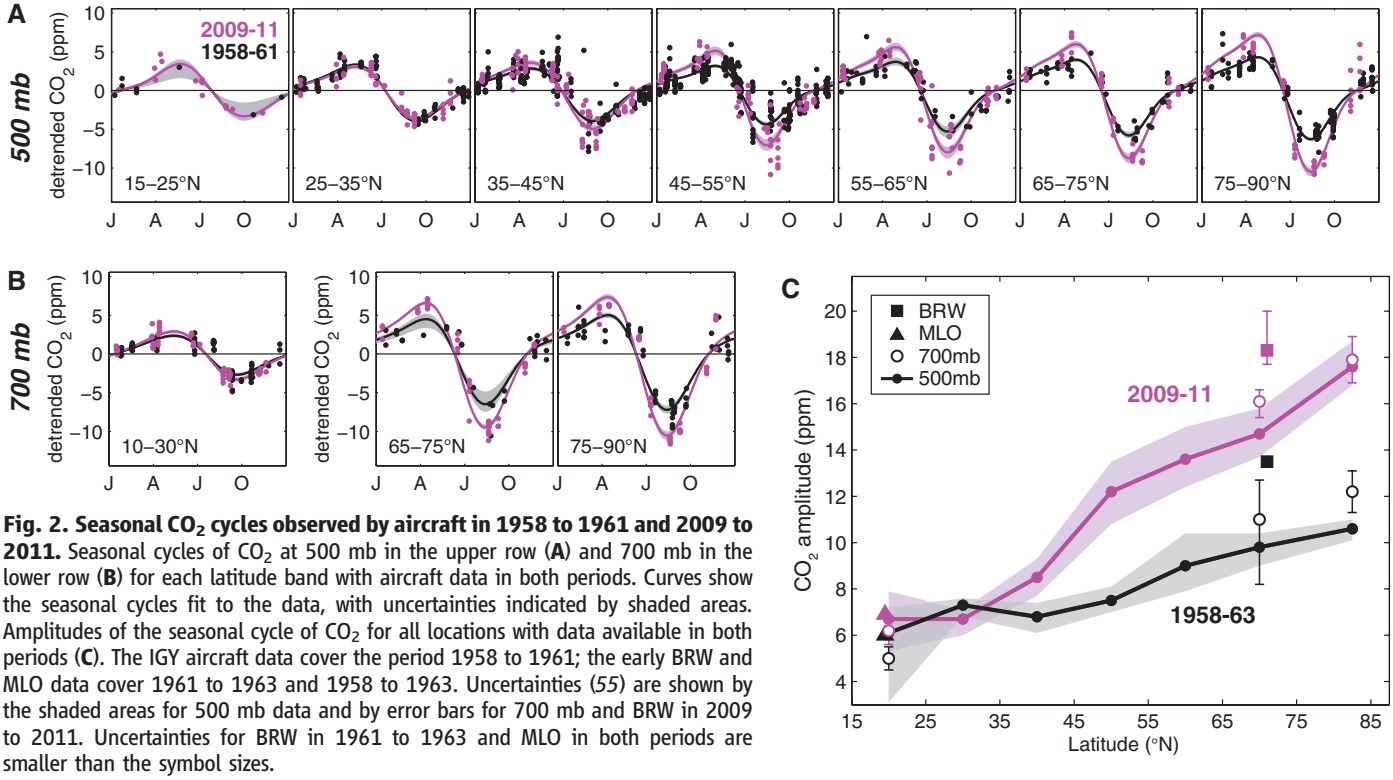

Fig. 2. Seasonal CO_2 cycles observed by aircraft in 1958 to 1961 and 2009 to 2011. Seasonal cycles of CO_2 at 500 mb in the upper row (**A**) and 700 mb in the lower row (**B**) for each latitude band with aircraft data in both periods. Curves show the seasonal cycles fit to the data, with uncertainties indicated by shaded areas. Amplitudes of the seasonal cycle of CO_2 for all locations with data available in both periods (**C**). The IGY aircraft data cover the period 1958 to 1961; the early BRW and MLO data cover 1961 to 1963 and 1958 to 1963. Uncertainties (*55*) are shown by the shaded areas for 500 mb data and by error bars for 700 mb and BRW in 2009 to 2011. Uncertainties for BRW in 1961 to 1963 and MLO in both periods are smaller than the symbol sizes.

Downloaded from www.sciencemag.org on September 13, 2013

temperate regions as well as Arctic and boreal regions results in an optimal increase of 53% (46 to 65% CI), assuming uniform change over these three regions (Case 2 in Fig. 3, D to F), or optimal zone-specific increases of 23% (12 to 42% CI) in the Arctic, 67% (57 to 87% CI) in the boreal, and 67% (54 to 89% CI) in the temperate region (Case 3 in Fig. 3, D to F).

Allowing for changes in the temperate region in Cases 2 and 3 improves the fit to high-latitude data compared to Case 1 while significantly decreasing the change attributed to Arctic and boreal regions. The simulations tend to produce fractional changes in amplitude that are more uniform with altitude than the observations, which show fractional changes in amplitude increase with height at high latitudes, and they tend to overestimate the CO_2 amplitude change at lower latitudes, which were not used in optimization. This may partly result from transport errors, caused by inaccuracies in modeled transport or unresolved transport changes since 1960, or from representation errors, caused by low resolution in the atmospheric transport models or in the terrestrial regions considered. Alternatively, the high-latitude effects on low-latitude CO_2 amplitudes may have been counteracted by decreasing NEP amplitudes in subtropical and tropical land regions. Fitting to all data and allowing for changes in subtropical and tropical NEP results in a change of –15% (–31 to 9% CI) in the tropics and subtropics (Case 4 in Fig. 3, D to F) without significantly affecting the optimal zone-specific NEP increases in the Arctic and boreal regions, though the NEP increase in the temperate region is reduced from Case 3.

The observations therefore require a widespread increase in the seasonal exchange of carbon in northern regions. Our analysis suggests that an additional 1.3×10^{15} to 2.0×10^{15} g carbon (Pg C) is exchanged with the atmosphere seasonally by Arctic, boreal, and temperate ecosystems combined in 2009 to 2011 compared with 1958 to 1963, an increase of 32 to 59%. This seasonal exchange represents the accumulation of carbon on land during the growing season (typically May to August) and the release of carbon during the dormant season, after subtracting annual mean exchange (*17*). Our analysis does not distinguish between enhanced growing season uptake and enhanced dormant season release, but changes in these two opposing fluxes may not necessarily be in balance. We do find, counter to previous studies invoking dormant or early growing season trends alone (*1*, *24*), that strong increases in CO_2 amplitude are unlikely to occur without enhanced uptake in the main growing season. This is because the intense fluxes in the main growing season (June and July) make a much larger contribution to the seasonal CO_2 amplitude than either the dormant season (September to April) or the shoulder seasons (May and August), as shown by calculations that examine contributions of the different seasons to the CO_2 cycle (*25*).

Enhancement in seasonal NEP is likely to be greatest in boreal regions, where all four cases require that the NEP amplitude changed by at least 53%. Less definitive is the requirement for decreased NEP amplitude in subtropical and tropical regions, although this may be consistent with the conversion of highly productive forests to crop or pasture lands and increased drought (*26*–*30*).

To explore potential mechanisms for changing NEP, we examine historical simulations of a subset of terrestrial ecosystem models currently participating in the fifth phase of the Coupled Model Intercomparison Project (CMIP5) (*31*). These models include simulations of CO_2 fertilization, climate change, and land use change, as well as nonlinear interactions between these processes; some additionally include dynamic vegetation

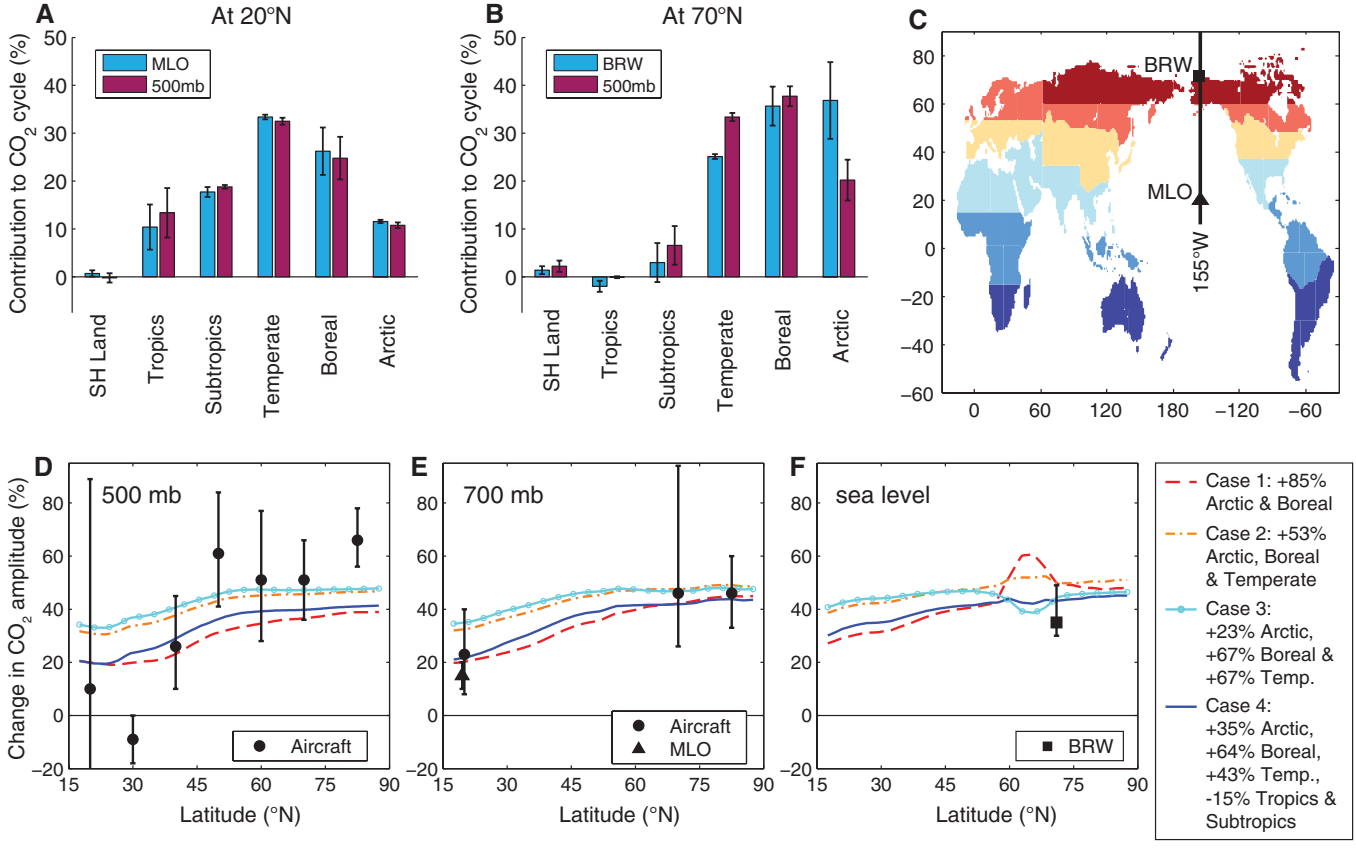

Fig. 3. Regional attribution of the seasonal CO_2 amplitude and its change over 50 years. Contributions of different terrestrial regions to the seasonal cycle of CO_2 at ground-based stations and at 500 mb for 20°N (**A**) and for 70°N (**B**) for 2009 to 2011, averaged over two atmospheric transport models, ACTM (*20*) and TM3 (*21*). Error bars reflect absolute differences between the two models. (**C**) Locations of the Mauna Loa and Barrow stations and the 155°W meridian, as well as the terrestrial regions considered. Arctic (red); boreal (orange); temperate (yellow); subtropics, tropics, and Southern Hemisphere land (shades of blue). (**D** to **F**) Change in CO_2 amplitude, in percentages, in the observations and in simulations where the amplitude in NEP was optimally scaled in different regions, plotted by latitude along 155°W for different pressures: (D) 500 mb aircraft data, (E) 700 mb aircraft data and Mauna Loa (670 mb), and (F) Barrow at sea level.

Downloaded from www.sciencemag.org on September 13, 2013

change, coupled nitrogen cycling, or simple crop modeling (*32*). We use the ACTM and TM3 atmospheric transport models to estimate atmospheric CO_2 amplitudes resulting from the CMIP5 models' simulated monthly NEP (Fig. 4).

None of the CMIP5 models can account for the increase in CO_2 amplitude north of 45°N at 500 mb between 1958 to 1961 and 2009 to 2011 (Fig. 4). Moreover, the recent CO_2 amplitude varies strongly between models, with a range of 6 to 19 ppm compared with the observed value of 13.8 ± 0.7 ppm. Previous studies have similarly shown that most terrestrial ecosystem models underestimate the long-term trend in CO_2 amplitude at Mauna Loa (*33*) and include large errors in the seasonal amplitude of NEP at eddy flux sites (*34*).

Simulated CO_2 amplitude changes from the CMIP5 models are nearly proportional to their NEP amplitude changes in northern ecosystems (*32*), as found in our optimization (Fig. 3), implying that the models underestimate the 50-year changes in NEP. This underestimate is not surprising, considering that the models' parameterizations of the direct effects of rising CO_2 and temperature are informed by laboratory and field studies that show low response to manipulations of CO_2 and temperature. Observed enhancement factors (*35*–*38*) suggest that the increase in net primary productivity (NPP) from the observed 50-year increases in CO_2 (23%) (*8*) and northern temperature (1.0°C north of 30°N) (*39*) should be no larger than 20 to 30%. Correspondingly, simulated increases in seasonal NPP amplitude are in the range 6 to 22% in the CMIP5 models, accompanied by higher amplitudes in heterotrophic respiration in most cases (*32*). Independent of the models, an explanation for the NEP changes based solely on a direct physiological response to warming is inconsistent with two features of the Barrow record (Fig. 1): (i) the weak interannual variability but strong long-term trend, and (ii) the increase in amplitude from the 1960s to the mid-1970s, a period when northern land temperatures did not rise but cooled slightly (*39*, *40*).

We are led to conclude that ecological changes in boreal and temperate forests are driving additional increases in the summertime uptake of carbon. This inference from atmospheric data is qualitatively consistent with expanding evidence for substantial changes occurring in these ecosystems. Forest inventories show increased stand area and biomass (*26*, *28*). Other ground-based studies show that evergreen shrubs and trees are migrating northward in response to warming (*41*–*43*), and that fire, logging, and other disturbances (*44*, *45*) are shifting the age composition toward younger, early-successional forests that experience shorter, more intense periods of seasonal carbon uptake (*46*, *47*). Satellite observations generally show trends toward increased greenness in northern ecosystems (*4*), although many areas of the boreal forest show browning trends in recent decades (*48*, *49*). The atmospheric evidence helps to quantify the aggregate effect of these, and other, types of ecological changes over the past 50 years. The changes are evidently underrepresented in the CMIP5 models, including those that allow for dynamic vegetation (Fig. 4) and coupled nitrogen cycling (Community Climate System Model 4 and Norwegian Earth System Model 1-M) (*50*).

The increase in seasonal CO_2 amplitude may be closely related to the net sink of CO_2 in northern extratropical land ecosystems that is currently ~2 Pg C year^{-1} (*28*, *51*–*53*). The relationship depends on how the sink has changed over time, which is not well constrained observationally but is likely to have increased since 1960 (*54*). Assuming that the sink was ~1 Pg C year^{-1} in 1960, the observed 1.3 to 2.0 Pg C year^{-1} increase in seasonal exchange over 50 years implies that growing season uptake increased by 40 to 60%, whereas dormant season release increased by only 20 to 50%, a result similar to the model scenarios described by Randerson *et al*. (*5*). A northern sink smaller than ~1 Pg C year^{-1} in 1960 would imply an even larger imbalance between growing season and dormant season trends.

There is no evidence that northern ecosystem trends are slowing down, because the largest CO_2 amplitudes at Barrow have been observed in the past few years (Fig. 1). The inability of the CMIP5 models to account for the observed increase in the amplitude of atmospheric CO_2 indicates that they underestimate the widespread ecological changes that occurred over the past 50 years and are likely to underpredict future changes.

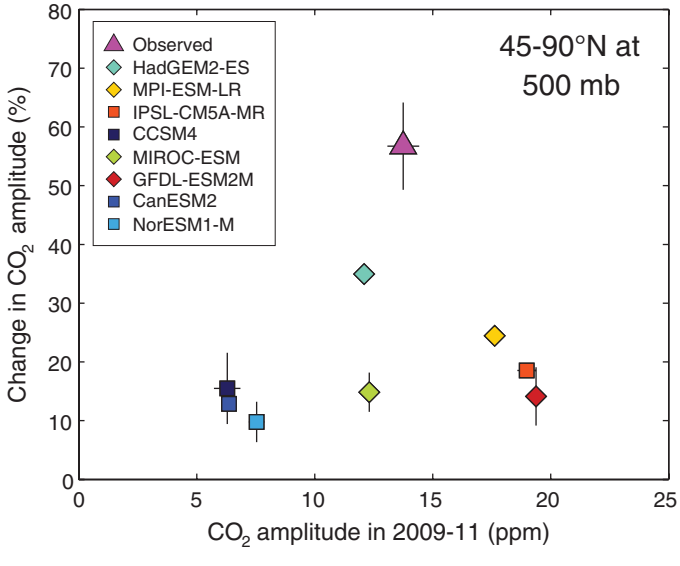

Fig. 4. Comparison of observations with CMIP5 model simulations. Change in amplitude of the seasonal cycle of CO_2 between 1958 to 1961 and 2009 to 2011 versus amplitude of the seasonal cycle for 2009 to 2011 at 500 mb, averaged over 45° to 90°N, in observations and in simulations of the CMIP5 land models (*56*) using the two atmospheric transport models, ACTM and TM3. Diamonds indicate models with dynamic vegetation. Error bars in the simulated amplitude and change in amplitude show differences between ACTM and TM3. The simulations include changes in fossil fuel emissions and atmospheric transport between 1958 to 1961 and 2009 to 2011. Oceanic fluxes were given by the two models' atmospheric CO_2 inversions for the late 2000s and held constant for the 1958 to 1961 and 2009 to 2011 periods.

References and Notes

1. C. D. Keeling, J. F. S. Chin, T. P. Whorf, *Nature* **382**, 146–149 (1996).
2. G. I. Pearman, P. Hyson, *J. Geophys. Res.* **86**, 9839 (1981).
3. R. B. Bacastow, C. D. Keeling, T. P. Whorf, *J. Geophys. Res.* **90**, 10529 (1985).
4. R. B. Myneni, C. D. Keeling, C. J. Tucker, G. Asrar R. R. Nemani, *Nature* **386**, 698–702 (1997).
5. J. T. Randerson, M. V. Thompson, T. J. Conway, I. Y. Fung, C. B. Field, *Global Biogeochem. Cycles* **11**, 535–560 (1997).
6. C. D. Keeling, *Tellus* **12**, 200–203 (1960).
7. J. J. Kelley, "An Analysis of Carbon Dioxide in the Arctic Atmosphere near Barrow, Alaska 1961 to 1967," Scientific Report of the Office of Naval Research, Contract N00014-67-A-0103-0007 NR 307-252 (1969).
8. R. F. Keeling, S. C. Piper, A. F. Bollenbacher, S. J. Walker, Atmospheric CO_2 records from sites in the SIO air sampling network. Trends: A Compendium of Data on Global Change (Carbon Dioxide Information Analysis Center, Oak Ridge National Laboratory, U.S. Department of Energy, Oak Ridge, TN, 2009).
9. K. W. Thoning, D. R. Kitzis, A. Crotwell, Atmospheric Carbon Dioxide Dry Air Mole Fractions from quasi-continuous measurements at Barrow, Alaska; Mauna Loa, Hawaii; American Samoa; and South Pole, 1973-2011, Version: 2012-05-07, available at ftp://ftp.cmdl.noaa.gov/ccg/co2/in-situ (2012).
10. Materials and methods are available as supplementary materials on *Science* Online.
11. See section SM1 in the supplementary materials.
12. S. C. Wofsy; HIPPO Science Team and Cooperating Modellers and Satellite Teams, *Philos. Trans. R Soc. A* **369**, 2073–2086 (2011).
13. C. D. Keeling, T. B. Harris, E. M. Wilkins, *J. Geophys. Res.* **73**, 4511–4528 (1968).
14. See section SM2 in the supplementary materials.
15. See section SM3 in the supplementary materials.
16. W. Bischof, B. Bolin, *Tellus* **18**, 155–159 (1966).
17. M. Heimann, C. D. Keeling, C. J. Tucker, *Geophys. Monogr. Ser* **55**, 277–303 (1989).
18. See section SM5 in the supplementary materials.
19. See section SM4 in the supplementary materials.
20. P. K. Patra *et al*., *Atmos. Chem. Phys.* **11**, 4163–4175 (2011).
21. C. Roedenbeck, S. Houweling, M. Gloor, M. Heimann, *Tellus B Chem. Phys. Meterol.* **55**, 488–497 (2003).
22. See sections SM6 and SM8 in the supplementary materials.
23. We specify the uncertainty in NEP amplitude change with 95% confidence intervals, assessed by varying parameters in the optimization and including jackknife estimates of the data.

Downloaded from www.sciencemag.org on September 13, 2013

24. S. A. Zimov *et al.*, *Clim. Change* **33**, 111–120 (1996).
25. See section SM7 in the supplementary materials.
26. FRA, "Global Forest Resources Assessment 2010" (Food and Agriculture Organization of the United Nations, Rome, 2010).
27. G. C. Hurtt *et al.*, *Clim. Change* **109**, 117–161 (2011).
28. Y. Pan *et al.*, *Science* **333**, 988–993 (2011).
29. O. L. Phillips *et al.*, *Science* **323**, 1344–1347 (2009).
30. K. R. Gurney, W. J. Eckels, *Tellus B Chem. Phys. Meterol.* **63**, 328–339 (2011).
31. K. E. Taylor, R. J. Stouffer, G. A. Meehl, *Bull. Am. Meteorol. Soc.* **93**, 485–498 (2012).
32. See section SM9 in the supplementary materials.
33. A. D. McGuire *et al.*, *Global Biogeochem. Cycles* **15**, 183–206 (2001).
34. K. Schaefer *et al.*, *J. Geophys. Res.* **117**, G03010 (2012).
35. L. Rustad *et al.*, *Oecologia* **126**, 543–562 (2001).
36. R. A. Houghton, *J. Geophys. Res.* **92**, 4223 (1987).
37. G. H. Kohlmaier *et al.*, *Tellus B Chem. Phys. Meterol.* **41**, 487–510 (1989).
38. R. J. Norby *et al.*, *Proc. Natl. Acad. Sci. U.S.A.* **102**, 18052–18056 (2005).
39. P. D. Jones *et al.*, *J. Geophys. Res.* **117**, D05127 (2012).
40. J. Hansen, R. Ruedy, M. Sato, K. Lo, *Rev. Geophys.* **48**, RG4004 (2010).
41. G. R. Walther *et al.*, *Nature* **416**, 389–395 (2002).
42. S. C. Elmendorf *et al.*, *Nat. Clim. Change* **2**, 453–457 (2012).
43. K. E. N. Tape, M. Sturm, C. Racine, *Glob. Change Biol.* **12**, 686–702 (2006).
44. A. J. Soja *et al.*, *Global Planet. Change* **56**, 274–296 (2007).
45. E. S. Kasischke *et al.*, *Can. J. Res.* **40**, 1313–1324 (2010).
46. S. A. Zimov *et al.*, *Science* **284**, 1973–1976 (1999).
47. L. R. Welp, J. T. Randerson, H. P. Liu, *J. Geophys. Res.* **111**, G03007 (2006).
48. S. J. Goetz, A. G. Bunn, G. J. Fiske, R. A. Houghton, *Proc. Natl. Acad. Sci. U.S.A.* **102**, 13521–13525 (2005).
49. D. Verbyla, *Glob. Ecol. Biogeogr.* **17**, 547–555 (2008).
50. P. E. Thornton, J.-F. Lamarque, N. A. Rosenbloom, N. M. Mahowald, *Global Biogeochem. Cycles* **21**, GB4018 (2007).
51. P. P. Tans, I. Y. Fung, T. Takahashi, *Science* **247**, 1431–1438 (1990).
52. K. R. Gurney *et al.*, *Nature* **415**, 626–630 (2002).
53. B. B. Stephens *et al.*, *Science* **316**, 1732–1735 (2007).
54. C. D. Keeling, S. C. Piper, T. P. Whorf, R. F. Keeling, *Tellus B Chem. Phys. Meterol.* **63**, 1–22 (2011).
55. We specify the uncertainty in CO_2 amplitude with 95% confidence intervals estimated using a jackknife procedure (fig. S3).
56. Only two models' simulations extended to 2011 (HadGEM2-ES and NorESM-1). Other models' output was available only through 2005, so NEP for 2009 to 2011 is given by the mean over 2001 to 2005. In these models, the change in NEP amplitude up to 2001 to 2005 may be 10% smaller than the change up to 2009 to 2011.

Acknowledgments: The Scripps CO_2 Program is supported by DOE grant DE-SC0005090. HIPPO was supported by NSF grants ATM-0628575, ATM-0628519, ATM-0628388, ATM-0628452, and ATM-1036399, and by the National Center for Atmospheric Research (NCAR). Recovery and updating of early aircraft, MLO, and BRW data was supported by NSF grant ATM-1036399. L.R.W. was supported by NASA award NNX11AF36G. Early observations at BRW were funded by U.S. Navy/Office of Naval Research contract N00014-67-A-0103-0007. Online access to all observational data is summarized in section SM10 of the supplementary materials. NCAR is supported by the NSF. Any opinions, findings, and conclusions or recommendations expressed in this material are those of the authors and do not necessarily reflect the views of NOAA, NSF, DOE or NASA. We thank the HIPPO science team and the crew and support staff at the NCAR Research Aviation Facility. We acknowledge the World Climate Research Programme's Working Group on Coupled Modelling, which is responsible for CMIP, and we thank the climate modeling groups for producing and making available their model output. Support of the CMIP data sets is provided by the Office of Science, U.S. Department of Energy. C. Roedenbeck provided assistance with the TM3 model. P.K.P. is partially supported by the Ministry of Education, Culture, Sports, Science and Technology Green Network of Excellence program. G.W.S. acknowledges support from the NSF Graduate Research Fellowship Program and the Environmental Protection Agency's Science to Achieve Results program.

Supplementary Materials

www.sciencemag.org/cgi/content/full/science.1239207/DC1
Materials and Methods
Figs. S1 to S9
Tables S1 to S7
References (*57*–*81*)

16 April 2013; accepted 17 July 2013
Published online 8 August 2013;
10.1126/science.1239207

Expanding the Fluorine Chemistry of Living Systems Using Engineered Polyketide Synthase Pathways

Mark C. Walker,[1]* Benjamin W. Thuronyi,[2]* Louise K. Charkoudian,[3]† Brian Lowry,[4] Chaitan Khosla,[3,4,5] Michelle C. Y. Chang[1,2]‡

Organofluorines represent a rapidly expanding proportion of molecules that are used in pharmaceuticals, diagnostics, agrochemicals, and materials. Despite the prevalence of fluorine in synthetic compounds, the known biological scope is limited to a single pathway that produces fluoroacetate. Here, we demonstrate that this pathway can be exploited as a source of fluorinated building blocks for introduction of fluorine into natural-product scaffolds. Specifically, we have constructed pathways involving two polyketide synthase systems, and we show that fluoroacetate can be used to incorporate fluorine into the polyketide backbone in vitro. We further show that fluorine can be inserted site-selectively and introduced into polyketide products in vivo. These results highlight the prospects for the production of complex fluorinated natural products using synthetic biology.

The catalytic diversity of biological systems provides enormous potential for application of living cells to the scalable production of pharmaceuticals, fuels, and materials (*1*–*4*). However, the scope of innovation of living organisms is typically limited to functions that confer a direct advantage for cell growth, thereby maximizing biomass as the end product rather than a distinct molecule or reaction of interest. In contrast, synthetic biology approaches allow us to disconnect some of these biochemical transformations from cell survival and reconnect them in different ways for the targeted synthesis of alternative classes of compounds. One particularly interesting area of opportunity is the development of methods to introduce fluorine into complex small-molecule scaffolds, which has become a powerful strategy for the design of synthetic pharmaceuticals. Estimates indicate that 20 to 30% of drugs, including many of the top sellers, contain at least one fluorine atom (*5*–*7*). Recent innovations have expanded the scope of synthetic C–F bond-forming methodologies, but the unusual elemental properties of fluorine that serve as the basis for its success also continue to restrict the range of molecular structures that can be accessed (*8*–*11*). As such, the invention of alternative routes for the site-selective introduction of fluorine into structurally diverse molecules, particularly under mild conditions, remains an outstanding challenge.

In comparison to synthetic small molecules, fluorine has limited distribution in naturally occurring organic compounds; the only organofluorine natural products characterized to date consist of a small set of simple molecules associated with the fluoroacetate pathway of *Streptomyces cattleya*, a soil bacterium that has the ability to catalyze the formation of C–F bonds from aqueous fluoride (Fig. 1A) (*12*, *13*). Although these compounds lack the intricacy typically expected of secondary metabolites, they represent a potentially rich source of modular organofluorine building blocks for the production of complex fluorinated natural products. In this regard, the backbones of several large classes of medicinally relevant natural products—including polyketides, isoprenoids, steroids, alkaloids, eicosanoids, leukotrienes, and others—are biosynthesized directly from the assembly and tailoring of simple acetate units (Fig. 1A). Introduction of the fluoroacetate monomer in place of acetate would allow us to incorporate fluorine into the backbone of these targets and create new molecular function by combining the medicinal

[1]Department of Molecular and Cell Biology, University of California, Berkeley, Berkeley, CA 94720–1460, USA. [2]Department of Chemistry, University of California, Berkeley, Berkeley, CA 94720–1460, USA. [3]Department of Chemistry, Stanford University, Stanford, CA 94305, USA. [4]Department of Chemical Engineering, Stanford University, Stanford, CA 94305, USA. [5]Department of Biochemistry, Stanford University, Stanford, CA 94305, USA.

*These authors contributed equally to this work.
†Present address: Department of Chemistry, Haverford College, Haverford, PA 19041, USA.
‡Corresponding author. E-mail: mcchang@berkeley.edu

Downloaded from www.sciencemag.org on September 13, 2013